Nanoscale

PAPER

Cite this: *Nanoscale*, 2016, **8**, 9310

Electroresponsive nanoparticles for drug delivery on demand

Devleena Samanta,† Niloufar Hosseini-Nassab† and Richard N. Zare*

Received 4th March 2016,
Accepted 12th April 2016

DOI: 10.1039/c6nr01884j

www.rsc.org/nanoscale

The potential of electroresponsive conducting polymer nanoparticles to be used as general drug delivery systems that allow electrically pulsed, linearly scalable, and on demand release of incorporated drugs is demonstrated. As examples, facile release from polypyrrole nanoparticles is shown for fluorescein, a highly water-soluble model compound, piroxicam, a lipophilic small molecule drug, and insulin, a large hydrophilic peptide hormone. The drug loading is about 13 wt% and release is accomplished in a few seconds by applying a weak constant current or voltage. To identify the parameters that should be finely tuned to tailor the carrier system for the release of the therapeutic molecule of interest, a systematic study of the factors that affect drug delivery is performed, using fluorescein as a model compound. The parameters studied include current, time, voltage, pH, temperature, particle concentration, and ionic strength. Results indicate that there are several degrees of freedom that can be optimized for efficient drug delivery. The ability to modulate linearly drug release from conducting polymers with the applied stimulus can be utilized to design programmable and minimally invasive drug delivery devices.

Introduction

The advent of smart biomaterials offers the promise of revolutionizing drug delivery by allowing the design of localized and controlled drug delivery systems (DDSs). Using stimuli-responsive materials that release their payload in response to specific triggers, it is possible to enhance drug efficacy as well as overcome adverse effects associated with oral and parenteral drug delivery. Various DDSs that respond to pH change,[1,2] temperature,[3] oxidizing/reducing agents,[4] enzymes,[5] magnetic field,[6,7] light,[8,9] ultrasound[10,11] and electrical stimuli[12–14] have been heavily investigated over the past few decades. Many intelligent designs of DDSs based on hydrogels,[15] polymers,[16] and nanoparticles[17] have been proposed. Still, the challenge remains to develop a DDS in which the drug release is evoked by external stimuli, scales linearly with the applied stimulus, and can be adjusted in accordance with patient needs.[18,19] Successful implementation of such a system can significantly improve the treatment of chronic diseases that require precise doses of medication or periodic injections.

Electroresponsive DDSs are particularly attractive in this regard because electrical signals can be generated relatively easily, be accurately controlled, and be remotely applied, without using large, specialized, and complex equipment. Moreover, it is possible to develop programmable DDSs that allow repetitive dosing. Electroactive polymers such as electroerodible hydrogels[20,21] and conducting polymers[13] have been shown to release a wide array of bioactive molecules. Polypyrrole is one such carrier material of wide interest as it is biocompatible[22,23] and can be prepared in biodegradable forms.[24] Several charged biologically relevant molecules such as risperidone,[25] dexamethasone,[12] adenosine triphosphate,[26] and methotrexate,[27] can be released from thin films of polypyrrole.

The major disadvantage of thin films is low drug loading.[28] Although more drug can be incorporated into thicker films,[28] the majority of the release takes place from the surface, and it is difficult to discharge the molecules from within the bulk of the film.[28] It was shown by Luo *et al.*[29] that a nine-fold enhancement of drug release is possible by designing nanoporous films. Compared to films, nanoparticles have increased surface-to-volume ratio that allows higher drug loading. In addition, nanoparticles are advantageous as their properties can be tuned by changing their shape and size, and their amount can be easily scaled up.[30]

Considering these benefits of nanoparticles, we have synthesized polypyrrole nanoparticles (PPy NPs) loaded with different drugs. Initial feasibility tests demonstrated that PPy NPs embedded in a hydrogel can be used as an electroresponsive DDS.[31] *In vivo* experiments showed the absence of fibrous tissue encapsulation at optimal concentration of the PPy NPs. In addition, histological examination of the injection site tissue did not exhibit significant differences from the control group, confirming the biocompatibility of PPy NPs.[31]

Department of Chemistry, Stanford University, Stanford, CA 94305, USA.
E-mail: zare@stanford.edu
†These authors contributed equally to this work.

In this work, we explored the potential of PPy NPs to be used as a general DDS to deliver charged drugs. By using an improved synthesis method, we can increase the drug loading by more than four times compared to our previous report.[31] In order to build a robust DDS, we performed a systematic study of the effect of the electrical parameters as well as the effect of the media on the nanoparticles using fluorescein as a model compound. We examined the influence of current, voltage, time of application of stimulus, pH, ionic strength, temperature, and concentration of nanoparticles. Our results demonstrate that several factors must be taken into consideration and optimized for efficient drug release. Moreover, we show pulsed release with a linear profile for molecules with different degrees of hydrophilicity and size: fluorescein (FL), a model highly water-soluble compound, piroxicam (PX), a hydrophobic, anti-inflammatory non-steroidal small molecule drug, and insulin (INS), a high molecular weight polypeptide hormone. To the best of our knowledge, this is the first demonstration of pulsed release of a polypeptide such as insulin from PPy NPs.

Materials

Pyrrole (reagent grade, 98%), sodium dodecyl sulfate (ReagentPlus®, ≥98.5%), 35 wt% hydrogen peroxide H_2O_2, piroxicam (>98%), fluorescein sodium salt, FITC-labeled human insulin, Pur-A-Lyzer™ Dialysis Kits, Whatman® Anotop® 25 syringe filters, were purchased from Sigma Aldrich. Screen printed electrodes were purchased from Metrohm and Palmsens. Platinum wire electrodes (0.5 mm diameter, 7.5 cm length) and Ag/AgCl reference electrodes were purchased from BASi. Slide-A-Lyzer™ MINI Dialysis Devices (7 kDa MWCO) were purchased from ThermoFisher Scientific and EMD Millipore Amicon™ Ultra-0.5 Centrifugal Filter Units (30 kDa MWCO) were purchased from Fisher Scientific.

Methods

Synthesis of drug-loaded polypyrrole nanoparticles

All reactions and measurements were carried out in quadruplicate and at room temperature, unless mentioned otherwise. In a typical synthesis, 15 mg FL or PX were added to 5 mL of an aqueous solution, 0.1 M in SDS and 40 mM in HCl. After complete dissolution of FL/PX, 100 μL pyrrole were added and stirred, followed by 200 μL of 35 wt% hydrogen peroxide (H_2O_2). To ensure complete yield, the solution was stirred for 24 h.

2 mL of the nanoparticles were transferred to Pur-A-Lyzer™ Dialysis tubes (MWCO 3.5 kDa) and the tubes were then placed in 100 mL water (supernatant), with stirring for 24 h. The washed nanoparticles were pipetted out and kept in a 15 mL centrifuge tube. Their volume was adjusted to 4 mL with water. INS-PPy NPs were prepared by first synthesizing the PPy NPs, and then adding a 2 mg mL^{-1} solution of INS in PBS to the PPy NPs in a 1 : 1 ratio.

Calculation of drug loading

The drug loading was determined from the difference between the initial amount of drug added and the amount of drug found in the supernatant after washing the nanoparticles. 200 μL of the supernatant were placed in each of 4 wells in a Greiner flat-bottomed 96 well-plate. 0, 10, 20 and 30 μL of 10 μg mL^{-1} standard solution of FL in phosphate buffered saline (PBS) were added to the respective wells. The total volume was adjusted to 230 μL with PBS. In case of PX, standard solutions were prepared in water instead of PBS. The UV-Vis spectrum was monitored by a TECAN infinite M1000 plate reader between 250–500 nm for PX and 400–700 nm for FL. The absorbance maxima were plotted against the concentration of the added FL/PX. The initial concentration of FL/PX in the supernatant was given by the *x*-intercept of the line of best fit through the plotted points. From this, the drug loading was calculated to be about ~12–13 wt%.

Size measurements

The size of the nanoparticles was determined both by dynamic light scattering (DLS) and scanning electron microscopy (SEM). For DLS, 5 μL of the nanoparticles were diluted with 1 mL of water and vortexed. The resultant solution was used to take the reading. The number of measurements per reading was set to 11, and each sample was read thrice using a Malvern Zetasizer Nano ZS90 instrument. For SEM, 10 μL of the solution were placed on an aluminum SEM stub and dried overnight. The sample was then sputter coated with Au/Pd and imaged with a Zeiss Sigma FESEM instrument.

Calibration curve for FL, PX, and INS

For FL, a 2.5 μg mL^{-1} solution was prepared in water. In a well 96-well plate, 20, 40, 60, 80 and 100 μL of this diluted solution were placed in 5 wells. The volume of each well was adjusted to 100 μL, followed by addition of 100 μL of 0.1 N NaOH. The absorbance was recorded between 400–700 nm. A similar procedure was followed for INS, except the starting concentration of INS in water was 20 μg mL^{-1}. As the INS used was FITC-labeled, its concentration could be easily calculated by measuring the absorbance of the solution. For PX, a 1 mg mL^{-1} solution was prepared by dissolving 3 mg PX in 1 mL 0.1 N NaOH. 800 μL water and 100 μL 0.1 N HCl were added to 100 μL of the solution to prepare a 100 μg mL^{-1} solution. The solution was diluted further with water to obtain a 10 μg mL^{-1} solution. 20, 40, 60, 80 and 100 μL of this diluted solution were placed in 5 wells. The volume of each well was adjusted to 100 μL with water and then 100 μL 0.1 N HCl were added to each well. The absorbance was recorded between 250–500 nm. For each molecule, the absorbance maxima were plotted as a function of the concentration, and these points were fit to a straight line by simple linear regression to get the final calibration curve.

Electrically stimulated drug release

Experiments were performed either using a screen printed electrode or using conventional three electrodes. For each

experiment in which an electrical stimulus was applied, a control experiment was performed in the absence of the stimulus to compare the results.

Effects of current, voltage, and time

Washed FL-PPy NPs were mixed with PBS at pH 7.4 in a 1 : 1 ratio and vortexed. 10 μL of the resulting solution were placed on a screen printed electrode (SPE) with carbon working and counter electrode, and Ag/AgCl reference electrode, covering all three electrodes. The appropriate current/voltage was applied for a given period of time. After this, 100 μL water were added to the SPE and mixed well with the solution on its surface. 100 μL of the mixture were retrieved and placed in a 30 kDa MWCO EMD Millipore Amicon™ Ultra-0.5 centrifugal filter unit. Another 100 μL water were added to the remaining solution on the SPE, mixed, retrieved, and placed in the same centrifugal unit. The filter was centrifuged at 10 000 rpm using an Eppendorf Centrifuge 5415*C* for 3 min. 100 μL of the filtrate were placed in a Greiner 96-well plate to which 100 μL 0.1 N NaOH were added. The absorbance reading was taken between 400–700 nm.

To test the effect of current, −50 μA, −100 μA, −200 μA, and −300 μA were applied for 25 s. In case of voltage, −0.5 V, −0.75 V, −1 V, −1.25 V, and −1.37 V were applied for 3 min. For time, −100 μA were applied for 25 s, 50 s, and 75 s.

Effect of particle concentration

The concentration of the washed nanoparticles was arbitrarily assigned a value of 1. These nanoparticles were then diluted with water to produce three solutions that were 3/4, 1/2, and 1/3 of the initial concentration, respectively. At each concentration, the nanoparticles were mixed in a 1 : 1 ratio with PBS 1 X at a pH 7.4. 10 μL of the solution were placed on the SPE. Thereafter, the experiment was carried out as described before for current, voltage, and time measurements. As stimulus, −200 μA were applied for 25 s.

Effects of temperature and pH

Washed FL-PPy NPs were diluted to 1/5 the concentration with water. 200 μL of this diluted solution were placed in a Slide-A-Lyzer™ MINI Dialysis Device (7 kDa MWCO). A coiled Pt wire electrode (0.5 mm diameter, 7.5 cm length) was placed in the dialysis cup as a working electrode. A Pt counter electrode and a Ag/AgCl reference electrode placed outside. These three electrodes were then immersed in a small glass vial containing 5 mL BR buffer at the pH of interest. As a stimulus, −1 V was applied for 3 min. Thereafter, 100 μL of the solution in the dialysis cup were mixed with 200 μL water and centrifuged at 10 000 rpm for 3 min using a 30 kDa MWCO EMD Millipore Amicon™ Ultra-0.5 centrifugal filter unit. 100 μL of the filtrate were placed in a Greiner 96-well plate. After adding 100 μL 0.1 N NaOH, the absorbance reading was taken between 400–700 nm.

To test the effect of pH, Britton–Robinson (BR) buffer was used. BR buffer is composed of a mixture of 0.04 M H_3BO_3, 0.04 M H_3PO_4, and 0.04 M CH_3COOH. 0.2 M NaOH was used to titrate the buffer to the desired pH. The buffer was prepared at three pH values: 5, 7.4, and 9. To test the effect of temperature, the experiments were performed at 3 temperatures: 0 °C, room temperature (23 °C), and 37 °C. BR buffer at a pH of 7.4 was used. At each temperature, all the reagents were equilibrated for 1 h prior to the experiment. An ice-bath was used to maintain 0 °C. A heated water-bath was used to maintain 37 °C.

Effect of ionic strength

Washed FL-PPy NPs were mixed in a 1 : 1 ratio with NaCl solutions of concentrations 8, 40, 100, 200, and 300 mM. 20 μL of the solution were placed on a SPE. −1.7 V for 30 s was applied as stimulus. 10 μL of the stimulated solution was diluted with 740 μL water and filtered using a 20 nm cutoff Whatman® Anotop® 25 syringe filter. 100 μL of the resulting solution were taken a well-plate and 100 μL 0.1 N NaOH were added and the absorbance was read between 400–700 nm.

Pulsed release of FL, PX, and INS

FL-PPy NPs and PX-PPy NPs were separately mixed with PBS 1 X at a pH of 7.4 in a 1 : 1 ratio. 30 μL of the resulting solution were placed on a SPE. After stimulation with p pulses (p = 1–3), 10 μL of the solution was sampled and diluted with 190 μL of water. It should be noted that for $p > 1$, the sampling was performed at the end of the last pulse, and not in between pulses. A similar protocol was followed for INS. The ratio of the volume of the solution stimulated to the surface area of the electrode was optimized for the Palmsens SPE. 15 μL of the stimulated solution was sampled and diluted with 300 μL water. For all compounds, 200 μL of the diluted sample was filtered by centrifugation at 10 000 rpm using a 30 kDa MWCO EMD Millipore Amicon™ Ultra-0.5 centrifugal filter unit. 100 μL of the filtrate were placed in a Greiner 96-well plate. 100 μL 0.1 N NaOH were added to this in case of FL and INS whereas 100 μL 0.1 N HCl were added in case of PX. The absorbance reading was taken between 400–700 nm for FL and INS, and 250–500 nm for PX. As a pulse, −100 μA was applied for 30 s, in case of FL and PX. Multiple pulses were applied 30 s apart. For INS, pulses of −1 V for 4 min were applied 10 s apart.

Graphs and figures

The data points plotted on all the graphs are the averages of n replicate measurements. The value of n is mentioned in each figure caption. Error bars correspond to one standard deviation.

Results and discussion

Synthesis and characterization

PPy NPs were synthesized in one step *via* a microemulsion technique described before,[32,33] using sodium dodecyl sulfate (SDS) as a surfactant and hydrogen peroxide as the oxidizing agent. This method avoids using metal-based strong oxidizing

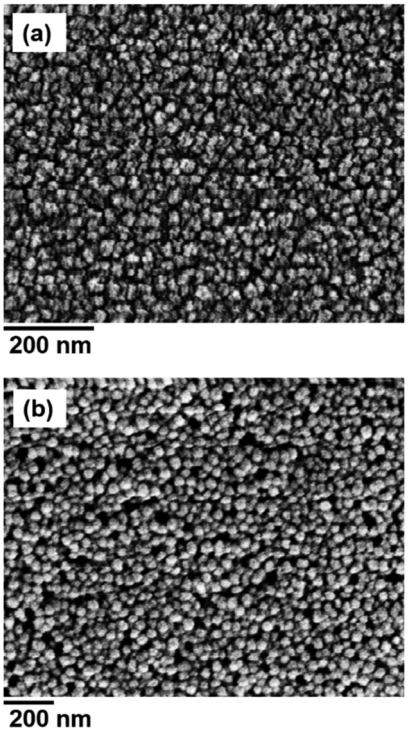

Fig. 1 SEM images of (a) FL-PPy and (b) PX-PPy.

agents which may leave toxic residue embedded within the nanoparticles.[32,34] FL and PX were loaded *in situ*, during the polymerization of pyrrole. INS was loaded after synthesis of the PPy NPs. The resulting nanoparticles were spherical, highly monodisperse, and stable in solution. FL-loaded nanoparticles (FL-PPy) were ~34 nm in size, whereas, PX-loaded nanoparticles (PX-PPy) were ~43 nm. These numbers correspond to the hydrodynamic diameters measured by dynamic light scattering and are in excellent agreement with size estimated by SEM (Fig. 1). INS-loaded nanoparticles (INS-PPy) were similar in size. The colloidal properties and stability of these nanoparticles have been investigated in detail in our previous publication.[33] The drug loading on the particles is ~13 wt%, which is a fourfold increase over that attained by a previous alternate synthetic route.[31] This value is not optimal, and can be further increased. However, in this work, our focus was to study the general parameters that affect drug release rather than optimize the system for the specific molecules tested. It should be noted that fluorescein disodium salt is highly water soluble (solubility: 500 g L^{-1} at 20 °C)[35] whereas piroxicam is hydrophobic (solubility: 23 mg L^{-1} at 22 °C).[36] We found that both compounds are easily incorporated into the PPy NPs.

Mechanism of drug release

Studies have shown that polypyrrole prepared under acidic conditions is in a partially oxidized state and has a positively charged backbone.[32] Drugs are attached to PPy NPs by a combination of electrostatic and hydrophobic interactions.[33] It has been suggested that drug release on electrical stimulation is caused by partial oxidation and reduction of the polymer.[28] Negatively charged drugs are released by reduction, whereas positively charged drugs are released by oxidation. In our case, as FL, PX, and INS are negatively charged, these compounds are expected to be released under reducing conditions according to the equation below, where D refers to the drug, x is the initial charge on the polymer, and y is the number of electrons pumped into the system by external stimulation:

$$\mathrm{PPy}^{x+}\cdot xD^- + ye^- \rightarrow \mathrm{PPy}^{(x-y)+}\cdot(x-y)D^- + yD^-$$

In contrast to a film, which is in direct contact with the electrode, the nanoparticles must diffuse to the surface of the working electrode to be able undergo a redox reaction. It is, therefore, important for efficient reduction of PPy NPs that the surface area of the electrode (A) be sufficiently large compared to the volume (V) of the solution containing the particles.[37] Hence, the A/V ratio must be optimized in order to maximize drug release from electrical stimulation and allow detection of the released drug. To satisfy this requirement, we designed two different setups. In the first one (Fig. 2a), screen printed electrodes (SPEs) with a circular carbon working electrode (diameter 4 mm) that allowed processing of volumes as low as 10 μL were used. Given that a large number of experiments were carried out, SPEs gave the added advantage of faster handling and lower required amount of nanoparticles in solution. In the other setup (Fig. 2b), a standard three-electrode system was used, in which the nanoparticles were confined to the vicinity of the working electrode in a dialysis cup with a semi-permeable membrane that allows the drug to pass through, but not the nanoparticles. The conventional three-electrode system was used in situations where SPEs did not provide sufficient control over the parameters. For instance, in the absence of a special setup, the effect of temperature cannot be studied using a SPE as it is difficult to control the temperature of a 10 μL drop.

Effects of current, time, and voltage

Once the appropriate A/V ratio was determined, we studied the effect of voltage, current, and time. We performed our experiments with a mixture of FL-PPy NPs and phosphate buffered saline (PBS) 1 X at a pH 7.4. PBS was used as it is isotonic and representative of the physiological pH. We found that FL release is linear with current and time (Fig. 3a and b). This behavior can be easily understood assuming faradaic conditions in which the amount of drug released is proportional to the extent of reduction of polypyrrole, which is in turn proportional to the total charge passed.

To investigate the effect of voltage, we studied drug release at 5 different voltages between −0.5 V and −1.37 V. It can be seen from Fig. 3c that the drug release is initially linear with the applied voltage, and beyond −1 V, nonlinearity sets in. We can understand this behavior by measuring the final current at each of these voltages. We note that in Fig. 3c the drug release closely mirrors the current profile, which is ohmic before −1 V

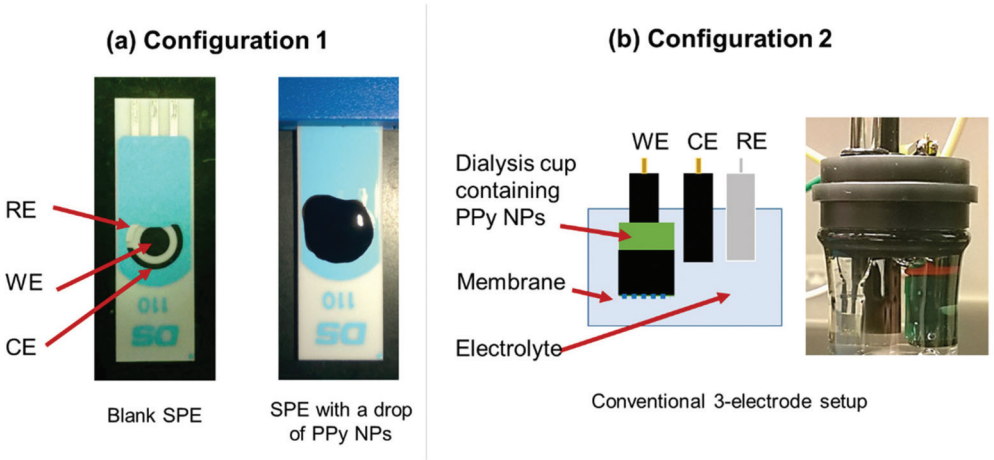

Fig. 2 Experimental setups for electrochemical drug release: (a) configuration 1: using screen printed electrode (SPE); (b) configuration 2: using a conventional three-electrode system.

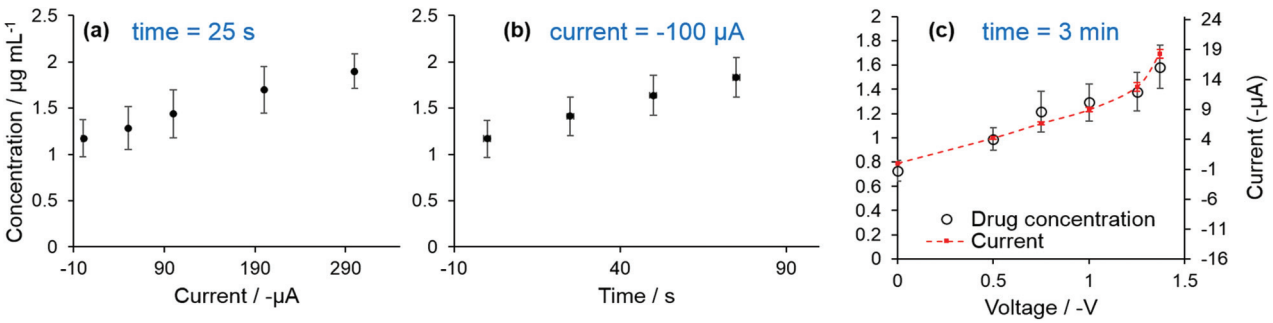

Fig. 3 Effect of (a) current, (b) time and (c) voltage on drug release (n = 4).

and sharply increases after that. This observation can be explained by the splitting of water (standard reduction potential of −1.04 V *vs.* Ag/AgCl[37]) which leads to the formation of hydroxyl ions at the working electrode, with simultaneous evolution of hydrogen.

Our previous study has shown that PPy NPs are pH sensitive, and negatively charged drugs are released more at higher pH.[33] The formation of hydroxyl ions owing to electrolysis of water increases the local pH around the working electrode and may also assist with drug release.[38] Therefore, current, voltage, and time are equally important for optimal drug release. In general, increased currents and voltages and longer application times lead to more drug release. However, at very high voltages, the drug might be susceptible to degradation unless the electrical pulse is short in duration. Higher voltages are also not preferable as they may lead to undesirable side reactions in more complex media in the body. Nonetheless, a high current/voltage applied for a short period of time may be helpful for cases that need immediate release of drugs. On the other hand, where small but sustained amount of drug is required, a smaller current/voltage can be used for a longer period of time.

Effect of particle concentration

The extent of reduction should increase with increasing concentration of reactants, which in this case are the PPy NPs. After purification *via* dialysis, the nanoparticles were diluted to half their initial reaction concentration. This concentration is arbitrarily assigned a value of 1 and referred to as the "original concentration" of the washed nanoparticles. FL-PPy NPs were diluted to 3/4, 1/2, and 1/3 of their original concentration and mixed with PBS. We find a linear dependence on FL release with nanoparticle concentration (Fig. 4a). The results imply that in cases where it is necessary to increase drug release but avoid higher voltage/current, higher concentrations of PPy NPs can be used in conjunction with weak stimuli.

Effects of pH and ionic strength

Prior studies have shown that polypyrrole nanoparticles are pH responsive.[33,39] Consequently, the electrically stimulated drug release is not only dependent on the electrical parameters, but also heavily dependent on the nature of the surrounding solution and its composition. The effect of pH on electrically stimulated drug release has not been investigated, particularly

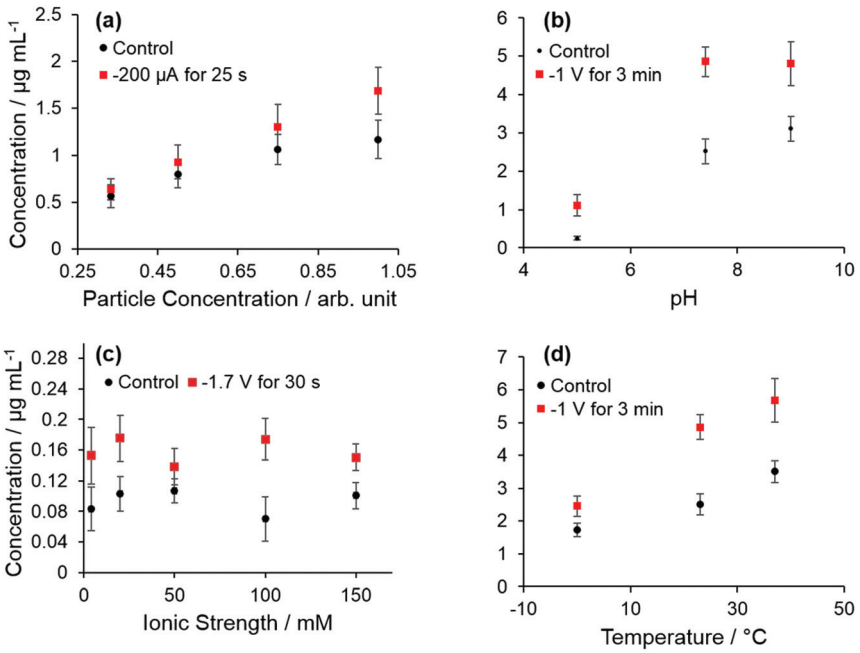

Fig. 4 Effect of (a) nanoparticle concentration, (b) pH, (c) ionic strength, and (d) temperature on drug release (n = 4).

in the case of nanoparticles. This effect is highly important as it can provide deeper insight into the mechanism of drug release and allow us to evaluate the applicability of a polypyrrole-based electrically controlled DDS at different locations of the body where the pH values are different.

While the physiological pH is rather constant around 7.4, the pH at some parts of the human body differ. For example, colon pH varies between 6.4–7.8 while sites of inflammation or cancerous tissue are more acidic (pH ~ 5–6).[2,40] To determine the effect of pH on drug release, we performed our experiments using configuration 2 as shown in Fig. 2b, at three different pH values: 5, 7.4, and 9. To maintain constant pH, Britton–Robinson (BR) buffer was used. This particular buffer was chosen because it can be prepared at different pH values over a wide range. Given that the same chemical species are involved in the preparation of the buffer, the introduction of errors that may arise from different ionic composition of the solution is prevented.

Fig. 4b shows that FL release in the absence of electrical stimuli is elevated at higher pH. This behavior is because hydroxyl ions reduce overall positive charge of the polypyrrole backbone and therefore its electrostatic interaction with the negatively charged drug is decreased as well.[33] On application of a constant voltage of −1 V *vs.* Ag/AgCl for 3 min, the drug release is increased at all pH values. However, we note that the relative magnitude of release upon electrical stimulation is higher at lower pH. That is, electrically stimulated drug release is about 4.4 times higher than free diffusion of drug at pH 5 but only 1.9 times higher at pH 7.4. A possible explanation could be that at lower pH, conductivity of polypyrrole is higher.[41] Increased conductivity facilitates higher drug release. Also, it has been suggested that in aqueous solutions, at higher pH, cation incorporation from the electrolytic solution may compete with anion ejection from the polymer upon reduction.[41,42]

Apart from pH, an important consideration is the ionic strength of the solution. It is preferable that a DDS is independent of ionic strength so that changes in ionic strength owing to movement of ions in and out of cells insignificantly alter the drug release. Physiological ionic strength is between 100–150 mM.[43] The FL-PPy NPs were mixed with NaCl solutions at different concentrations to prepare solutions with ionic strengths between 4–150 mM with respect to NaCl. We do not find any significant influence of ionic strength on drug release within the concentration range studied (Fig. 4c). The scatter seen in the graph arises from random fluctuations.

Effect of temperature

The human body temperature is nearly constant at 37 °C. An effective DDS must not be greatly influenced by small changes in temperature, as this can lead to faulty operation. We studied the drug release when −1 V is applied for 3 min at 0 °C, room temperature (23 °C) and 37 °C. In general, as the temperature increases, the amount of drug release increases for both stimulated and control samples (Fig. 4d). Free diffusion of the drugs is higher at elevated temperatures from decreased strength of interaction with the nanoparticle. Electrically triggered drug release increases as the conductivity of the solution increases. However, it is clear from Fig. 4d that small changes in temperature (less than 5 °C) do not significantly alter drug release. So, the proposed DDS system can tolerate minor temperature fluctuations, which may happen in the body, caused for example by fever.

Pulsed release of FL, PX, and INS

One of the key features of a controlled and programmable DDS is zero-order kinetics so that the drug release scales linearly with the applied stimulus. Also, the drug release should respond linearly to the application of multiples pulses of the same magnitude used for treatment of diseases that require repeated doses. From Fig. 5a, we see the amount of FL released from FL-PPy NPs increases linearly when multiple pulses of −100 μA for 25 s are applied. Therefore, PPy NPs have the desired properties mentioned above, which may be exploited to build a programmable DDS.

To test whether the generality of this procedure, we used PX-PPy NPs and INS-PPy NPs. Both PX and INS are typically administered in a repeated manner. PX is a small molecule drug used in the treatment of rheumatoid arthritis. INS is a high molecular weight polypeptide used in diabetes treatment. Given that patient nonadherence to medication required to treat long-lasting conditions can be as high as 40%,[44] these molecules could benefit from such a controllable DDS. Fig. 5a and b indicate that it is possible to release PX and INS in a pulsed manner. As PX is a small molecule, the stimulus applied as a pulse was maintained the same as that for FL. For INS, −1 V for 4 min was applied as a pulse.

The maximum percentage of drug that can be released on prolonged exposure to electrical stimulus depends on the nature of the drug, its charge, and the method of loading the drug. This number varied between 10% (for FL) to 60% (for INS). The more efficient release of INS could be possibly attributed to loading of INS outside the particles, unlike FL and PX. We are currently working on techniques to improve the magnitude of release.

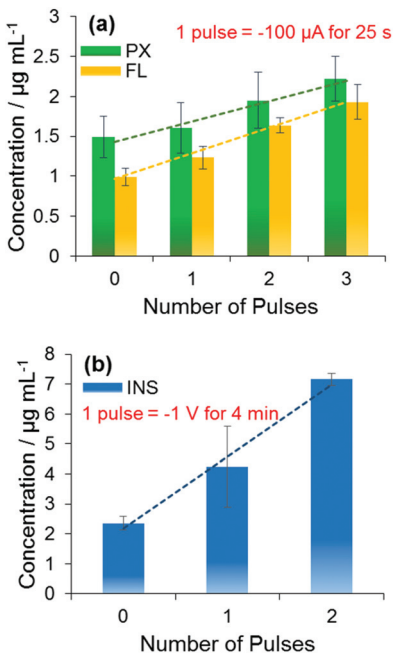

Fig. 5 Pulsed release of (a) FL (n = 4), PX (n = 3), and (b) INS (n = 3). Dotted lines show trends.

It should be noted that the three molecules tested here are starkly different from each other in terms of their hydrophilicity and molecular weight. Our results demonstrate PPy NPs can be potentially used as a general DDS, although the system will need to be optimized for each drug for efficient dosage control.

Conclusions

We have studied electroresponsive drug release from PPy NPs prepared by a facile one-step microemulsion synthesis using FL as a model compound. We have investigated the effects of electrical stimuli such as current, voltage, and duration of application, the influence of the solution composition, such as particle concentration, pH, and ionic strength, as well as, temperature of the system. Our results indicate that electrically stimulated drug release from PPy NPs is dependent on several parameters not previously considered, and these factors must be optimal for efficient drug release. Among these, the most important parameters are the current, voltage, and time. Drug release is observed at voltages as low as −0.5 V *vs.* Ag/AgCl reference electrode. For efficient passage of current, the key point is to ensure that the surface area of the electrode is large compared to the volume of the solution stimulated. Further, we have shown with FL, PX, and INS that repetitive and pulsed release with a linear response is possible. These results suggest that our DDS is general. We conclude that PPy NPs are promising for developing controlled and programmable drug delivery system for treatment of diseases that require repeated dosage of drugs. It should be possible to build minimally invasive drug delivery systems with miniaturized electronics that enable remotely controlled wireless drug delivery from these PPy NPs.

Acknowledgements

We are grateful to L. M. Joubert at The Cell Sciences Imaging Facility (CSIF), Stanford University, for helping with SEM imaging. DS thanks the Center for Molecular Analysis and Design (CMAD), Stanford University, and the Stanford Graduate Fellowship, for funding.

References

1 J. Y. Lee, S. J. Chung, H. J. Cho and D. D. Kim, *Adv. Funct. Mater.*, 2015, **25**, 3705–3717.
2 V. Balamuralidhara, T. M. Pramodkumar, N. Srujana, M. P. Venkatesh, N. Vishal Gupta, K. L. Krishna and H. V. Gangadharappa, *Am. J. Drug Discovery Dev.*, 2011, **1**, 24–48.
3 M. Zhou, S. Liu, Y. Jiang, H. Ma, M. Shi, Q. Wang, W. Zhong, W. Liao and M. M. Q. Xing, *Adv. Funct. Mater.*, 2015, **25**, 4730–4739.

4 K. Wang, Q. Hu, W. Zhu, M. Zhao, Y. Ping and G. Tang, *Adv. Funct. Mater.*, 2015, **25**, 3380–3392.
5 R. de la Rica, D. Aili and M. M. Stevens, *Adv. Drug Delivery Rev.*, 2012, **64**, 967–978.
6 C. S. S. R. Kumar and F. Mohammad, *Adv. Drug Delivery Rev.*, 2011, **63**, 789–808.
7 C. Sun, J. S. Lee and M. Zhang, *Adv. Drug Delivery Rev.*, 2008, **60**, 1252–1265.
8 S. Park, W. Park and K. Na, *Adv. Funct. Mater.*, 2015, **25**, 3472–3482.
9 C. P. McCoy, C. Rooney, C. R. Edwards, D. S. Jones and S. P. Gorman, *J. Am. Chem. Soc.*, 2007, **129**, 9572–9573.
10 K. W. Ferrara, *Adv. Drug Delivery Rev.*, 2008, **60**, 1097–1102.
11 J. L. Paris, M. V. Cabanas, M. Manzano and M. Vallet-Regi, *ACS Nano*, 2015, **9**, 11023–11033.
12 R. Wadhwa, C. F. Lagenaur and X. T. Cui, *J. Controlled Release*, 2006, **110**, 531–541.
13 D. Svirskis, J. Travas-Sejdic, A. Rodgers and S. Garg, *J. Controlled Release*, 2010, **146**, 6–15.
14 F. Fantozzi, E. Arturoni and R. Barbucci, *Bioelectrochemistry*, 2010, **78**, 191–195.
15 A. Kikuchi and T. Okano, *Adv. Drug Delivery Rev.*, 2002, **54**, 53–77.
16 Y. Bae and K. Kataoka, *Adv. Drug Delivery Rev.*, 2009, **61**, 768–784.
17 I. I. Slowing, B. G. Trewyn, S. Giri and V. S. Y. Lin, *Adv. Funct. Mater.*, 2007, **17**, 1225–1236.
18 X. Huang and C. S. Brazel, *J. Controlled Release*, 2001, **73**, 121–136.
19 C. Alvarez-Lorenzo, B. Blanco-Fernandez, A. M. Puga and A. Concheiro, *Adv. Drug Delivery Rev.*, 2013, **65**, 1148–1171.
20 D. Mawad, K. Gilmore, P. Molino, K. Wagner, P. Wagner, D. L. Officer and G. G. Wallace, *J. Mater. Chem.*, 2011, **21**, 5555–5560.
21 I. C. Kwon, Y. H. Bae and S. W. Kim, *Nature*, 1991, **354**, 291–293.
22 A. Ramanaviciene, A. Kausaite, S. Tautkus and A. Ramanavicius, *J. Pharm. Pharmacol.*, 2007, **59**, 311–315.
23 X. Wang, X. Gu, C. Yuan, S. Chen, P. Zhang, T. Zhang, J. Yao, F. Chen and G. Chen, *J. Biomed. Mater. Res., Part A*, 2004, **68**, 411–422.
24 G. Shi, M. Rouabhia, Z. Wang, L. H. Dao and Z. Zhang, *Biomaterials*, 2004, **25**, 2477–2488.
25 D. Svirskis, B. E. Wright, J. Travas-Sejdic, A. Rodgers and S. Garg, *Electroanalysis*, 2010, **22**, 439–444.
26 M. Pyo and J. R. Reynolds, *Chem. Mater.*, 1996, **8**, 128–133.
27 N. Alizadeh and E. Shamaeli, *Electrochim. Acta*, 2014, **130**, 488–496.
28 B. Alshammary, F. C. Walsh, P. Herrasti and C. Ponce de Leon, *J. Solid State Electrochem.*, 2015, 1–21.
29 X. Luo and X. T. Cui, *Electrochem. Commun.*, 2009, **11**, 402–404.
30 G. M. Whitesides, *Nat. Biotechnol.*, 2003, **21**, 1161–1165.
31 J. Ge, E. Neofytou, T. J. Cahill, R. E. Beygui and R. N. Zare, *ACS Nano*, 2012, **6**, 227–233.
32 K. Leonavicius, A. Ramanaviciene and A. Ramanavicius, *Langmuir*, 2011, **27**, 10970–10976.
33 D. Samanta, J. L. Meiser and R. N. Zare, *Nanoscale*, 2015, **7**, 9497–9504.
34 S. P. Armes, *Synth. Met.*, 1987, **20**, 365–371.
35 http://www.chemicalbook.com/ChemicalProductProperty_EN_CB0753559.htm, 2015, 1. accessed Feb 2, 2016.
36 D. S. Wishart, C. Knox, A. C. Guo, D. Cheng, S. Shrivastava, D. Tzur, B. Gautam and M. Hassanali, *Nucleic Acids Res.*, 2008, **36**, D901–D906.
37 A. J. Bard and L. Faulkner, *Electrochemical Methods: Fundamentals and Applications*, Wiley, New York, 2001, vol. 417, pp. 808–810.
38 F. Boulmedais, C. S. Tang, B. Keller and J. Vörös, *Adv. Funct. Mater.*, 2006, **16**, 63–70.
39 D. Park, Y. Cho, S. H. Goh and Y. Choi, *Chem. Commun.*, 2014, **50**, 15014–15017.
40 J. Liu, Y. Huang, A. Kumar, A. Tan, S. Jin, A. Mozhi and X. J. Liang, *Biotechnol. Adv.*, 2013, **32**, 693–710.
41 Q. Xie, S. Kuwabata and H. Yoneyama, *J. Electroanal. Chem.*, 1997, **420**, 219–225.
42 M. R. Gandhi, P. Murray, G. M. Spinks and G. G. Wallace, *Synth. Met.*, 1995, **73**, 247–256.
43 J. D. Cortese, A. L. Voglino and C. R. Hackenbrock, *J. Cell Biol.*, 1991, **113**, 1331–1340.
44 L. R. Martin, S. L. Williams, K. B. Haskard and M. R. Dimatteo, *Ther. Clin. Risk Manage.*, 2005, **1**, 189–199.